Study with in situ data of the May and October 2024 geomagnetic storms

Alessandro Bemporad[1], Panagiota Ntavoultzopoulou[2], Giorgio Bergamin[1]

[1]INAF – Turin Astrophysical Observatory, Italy
[2]University of Ioannina, Greece

ABSTRACT

In this study, we analyzed two major geomagnetic storms that occurred in 2024. For our analysis, we used in-situ data from NASA's Advanced Composition Explorer (ACE) spacecraft, specifically measurements from the SWEPAM instrument. We examined key plasma parameters such as proton density, magnetic field components, and bulk speed, while also calculating derived quantities like Alfvén speed, the convection electric field, and the Alfvénic Mach number. Our analysis covered the time intervals from 09/05/2024 to 13/05/2024 for the May geomagnetic storm and from 09/10/2024 to 10/10/2024 for the October storm, focusing on their evolution in relation to the Dst index. This study was conducted as part of a two-month Erasmus internship.

1. Introduction

As defined by the COST Action 724, the space weather is "*the physical and phenomenological state of natural space environments. The associated discipline aims, through observation, monitoring, analysis and modeling, at understanding and predicting the state of the Sun, the interplanetary and planetary environments, and the solar and non-solar driven perturbations that affect them, and also at forecasting and nowcasting the potential impacts on biological and technological systems"*. The importance of studying space weather concerns understanding fundamental astrophysical events as well as solar-terrestrial interactions, which of course influence our planet. Some examples are high radiations impacting satellites, which can affect communication and navigation systems, geomagnetic storms causing electrical blackouts, high energy particles from solar storms increasing radiation levels threatening the life of the astronauts etc. In this report we focused on 2 geomagnetic storms that happened in May and in October 2024. As it is written in the NOAA's space weather prediction center website "*A geomagnetic storm is a major disturbance of Earth's magnetosphere that occurs when there is a very efficient exchange of energy*

*from the solar wind into the space environment surrounding Earth. These storms result from variations in the solar wind that produces major changes in the currents, plasmas and fields in Earth's magnetosphere" (*Figure 1*).*

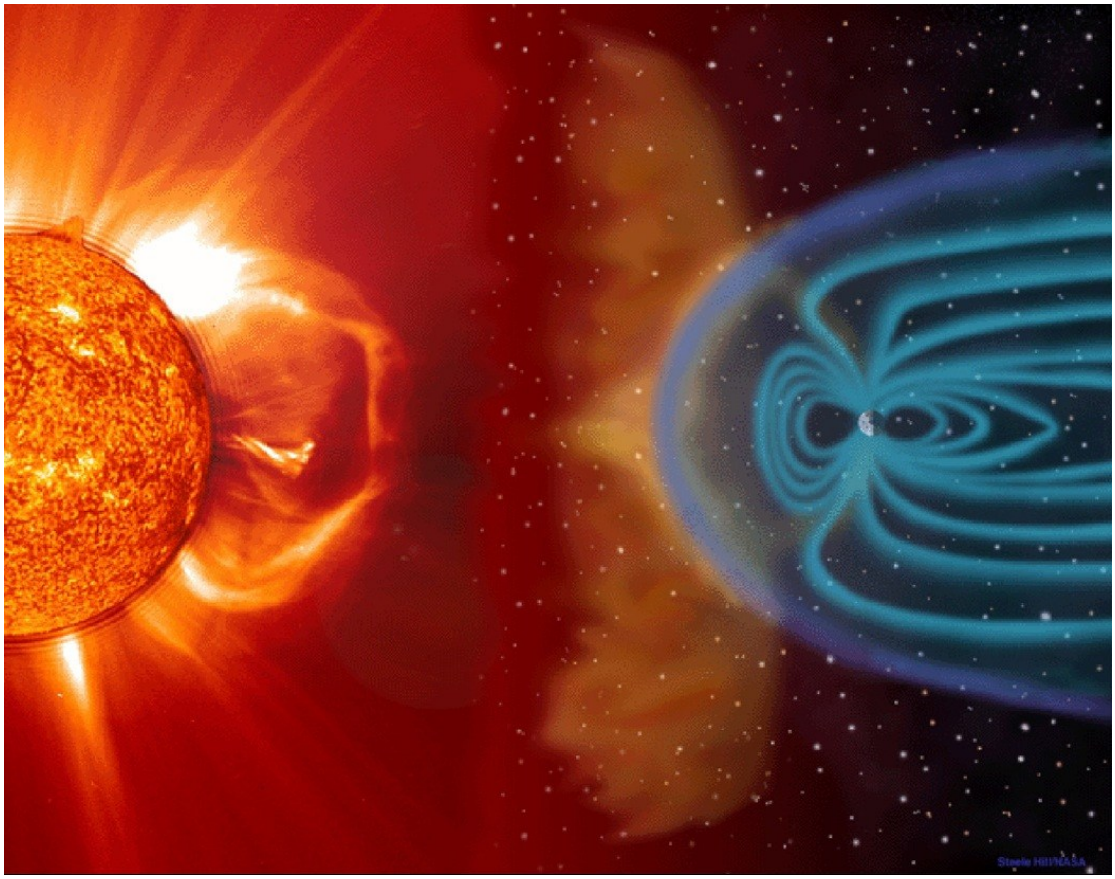

Figure 1: outreach artistic representation of the Sun-Earth interactions and protection offered by the Earth's magnetic field from the solar activity. Image by Steele Hill, NASA Goddard Space Flight Center.

For the May 2024 geomagnetic storm, as reported by spaceweather.com, multiple Interplanetary Coronal Mass Ejections (ICMEs) were ejected from the giant sunspot AR3664 on 09/05/2024 and were headed toward Earth. It was predicted that a so-called "Cannibal ICME"—a phenomenon resulting from the merging of multiple eruptions in interplanetary space—would strike Earth in the early hours of May 11th, triggering a G4-class storm.

On 10/05/2024, after the ICME impacted Earth's magnetosphere, the solar wind speed around our planet exceeded 700 km/s, and southward-pointing magnetic fields from the Sun created a "crack" in Earth's magnetosphere, likely due to magnetic reconnection between the magnetospheric and interplanetary magnetic fields. This event led to the most intense geomagnetic storm in over 20 years (G5-class), producing auroras visible even at low latitudes (Figure 2).

By 11/05/2024, the geomagnetic storm had subsided, but AR3664 remained highly active, measuring approximately 15 times the size of Earth. On 14/05/2024, this

sunspot unleashed the strongest solar flare of the current solar cycle, classified as X8.7, as measured by the GOES satellite. The flare began on 14/05/2024 at 01:46:00 UT, peaked at 16:51:00 UT, and ended at 17:02:00 UT (exact timing sourced from solarmonitor.com). Extreme ultraviolet radiation from this flare ionized the upper layers of Earth's atmosphere, causing a deep shortwave radio blackout over the Americas.

Figure 2: Aurora on 11th of May Photo by Gunjan Sinha.

For the October 2024 geomagnetic storm, on 08/10/2024, sunspot AR3848 was directly facing Earth when it released a powerful X1.8-class solar flare, as measured by GOES. The flare began on 09/10/2024 at 01:25:00 UT, peaked at 01:56 UT, and ended at 02:14:11 UT (exact timing sourced from solarmonitor.com).

On 09/10/2024, the Sun launched a CME directly toward Earth, causing a major "crack" in Earth's magnetic field and triggering geomagnetic storms fluctuating between G2 and G4-class. As a result, electrical currents flowed through rocks and soil in the United States, with peak voltages in the Midwest reaching nearly 5 V/km—two orders of magnitude higher than typical quiet conditions.

During the night of October 10-11, auroras were observed at very low latitudes. By 11/10/2024, the G4 geomagnetic storm had ended, and by 12/10/2024, Earth's magnetic field had largely returned to normal. This information was also reported by spaceweather.com.

The objective of this study was to characterize the in-situ data associated with these two geomagnetic storms to better understand their origins and analyze the evolution of various interplanetary plasma parameters during the exact dates of these events.

2. In situ data analysis

The data that we analyzed came from NASA's Advanced Composition Explorer (ACE). This spacecraft was designed to study energetic particles from the Sun- Earth Lagrange point L1 (about 1.5 million kilometers from Earth) and it collects and analyzes particles of solar, interplanetary, interstellar and galactic origins. More specifically, we used the in-situ data from these 2 scientific instruments: the Solar Wind Electron, Proton and Alpha Monitor (SWEPAM), and the Magnetometer (MAG). We used the values of these parameters for both geomagnetic storms: B_x, B_y, and B_z components from MAG, and the proton density n_p and bulk speed v_p from SWEPAM. For the geomagnetic storm in May, we downloaded the data from MAG and SWEPAM from 09/05/2024 to 14/05/2024, and for the one in October we downloaded the data from 09/10/2024 to 13/10/2024. These data have a cadence of 1 minute, so for each day we had 1440 different values for each parameter.

We also downloaded the data of the Dst-index from the World Data Center for Geomagnetism (WDC), Kyoto Data Analysis Center for Geomagnetism and Space Magnetism, which have a cadence of 1 hour. The Dst-index, from "disturbance storm time" is one of the indices that describes the strength of a geomagnetic storm, representing mostly the intensity of the ring currents around our planet. For the data analysis we used the IDL – Interactive Database Language.

For the first part of the analysis, we extracted the values of B_x, B_y, and B_z (measured in nT, components projected in the reference system shown in Figure 3) from the ACE MAG files, as well as the bulk speed (km s^{-1}) and the proton density (p cm^{-3}) from the ACE SWEPAM files. Then as a first step we corrected the missing values that the files contained, using the WHERE() function in IDL, making the missing values (labelled as -9999.9 and -999.9) equal to zero. Then, we calculated the total magnetic field strength, $B_{tot} = \sqrt{B_x^2 + B_y^2 + B_z^2}$, we converted the units of the total magnetic field from nT to Gauss, and computed the Alfvén Speed, $v_A = \frac{B_{tot}}{\sqrt{4\pi\rho}}$, with ρ (g cm^{-3}) being the mass density given by $\rho = n_p\, m_p$ (with m_p proton mass).

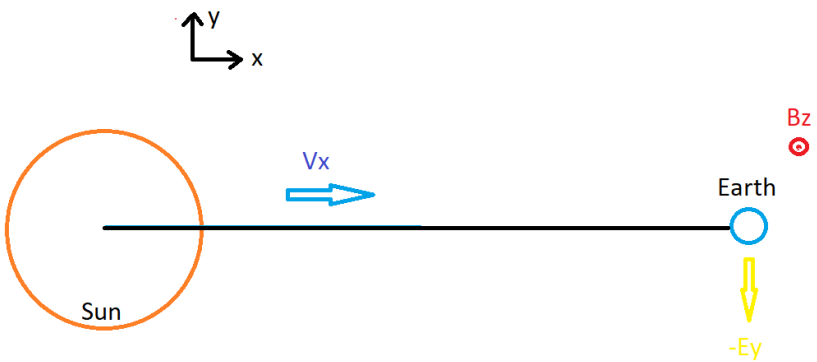

Figure 3 X,Y,Z axes in the reference system used in this work

We then moved on with an interpolation to all these extracted parameters from 1-minute cadence to 1-hour timestep to match the 1-hour cadence of the Dst values. In order to compare the time evolution of the interplanetary plasma parameters measured in L1 and the corresponding evolution of the Dst index, we also considered the time required for the propagation of interplanetary plasma from L1 to the Earth. For this purpose, we used the so-called "*flat time-shift method*" described by the following expression

$$t'_N = t_N + \frac{d}{v(t_N)},$$

where t_N is the time on Earth and $d = 1.5 \cdot 10^6$ km, $v_p(t_N)$ being the proton bulk speed at time t_N, and t_N' is the new interpolated time. In that way we align the ACE in situ data from L1 with the time of the Dst index that is being recorded on Earth. We also calculated the $\frac{Bz}{Btot}$ ratio in order to see the impacts of the solar wind on the Earth's magnetic field along the axis of their interaction.

We then calculated the convection electric field $\bar{E} = -\bar{v}_p \times \bar{B}$, where B is the vector of the magnetic field (nT), and v_p is the vector of the proton velocity (km s^{-1}). Now we explicit all the components of B and v_p:

$$\bar{E} = -(v_x\,, \quad v_y\,, \quad v_z) \times (B_x\,, \quad B_y\,, \quad B_z)$$

and for the cross product we have:

$$\bar{E} = (E_x\ , E_y\ , E_z) = (B_y\, v_z - B_z\, v_y\ , B_z\, v_x\ - B_x\, v_z\ , B_x\, v_y\ - B_y\, v_x).$$

Starting from the above general expression, some considerations need to be made. First of all, in our SR, the solar wind plasma velocity is almost entirely parallel to the x-axis, hence $v_y \approx v_z \approx 0$; then we obtain

$$\bar{E} = (0\ , B_z\, v_x\ , -B_y\, v_x).$$

Among these two remaining non-zero components, the component $E_z = - B_y\, v_x$ is usually neglected in the study of geomagnetic storms, and only the component $E_y = v_x\, B_z$ of the convection electric field is primarily considered because it plays a crucial role in magnetic reconnection and energy transfer from the solar wind to Earth's magnetosphere. In fact, the Earth's magnetosphere is dominated by a dipolar magnetic field, which is primarily oriented along the north-south direction (parallel to the *z*-axis). When the solar wind arrives with its interplanetary magnetic field, the B_z component is thus the most relevant for magnetic reconnection at the magnetopause (the boundary between the solar wind and the magnetosphere). In particular:

- If $B_z > 0$ (northward direction), the interplanetary magnetic field is aligned with Earth's magnetic field, reducing the efficiency of magnetic reconnection;

- If $B_z < 0$ (southward direction), the interplanetary magnetic field is anti-aligned with Earth's magnetic field, facilitating magnetic reconnection at the magnetopause. This allows solar wind plasma to enter the magnetosphere, triggering geomagnetic storms.

Hence, while there is also a component $E_z = -B_y v_x$, it is not as influential in geomagnetic storms because it does not directly drive the main magnetic reconnection between the solar wind and the magnetosphere, and the electric field associated with B_y has a more localized effect on the magnetospheric structure but is not the primary driver of solar wind-magnetosphere coupling.Lastly, we calculated also the Alfvènic Mach number (M_A), which is the ratio of bulk speed (v_p) and the Alfvén speed (v_A). When $M_A < 1$ the magnetic field dominates over the motion of the plasma, and the plasma flow is sub-Alfvenic. When $M_A > 1$ the plasma flow is super-Alfvénic, and in this case the plasma flow speed is larger than the magnetic wave propagation speed, leading to magnetohydrodynamic (MHD) shocks.

3. The May 2024 storm

A summary of various plasma parameters and the Dst index is provided in Figure 4. In this figure, the *x*-axis represents time in hours, with zero corresponding to 00:00 on 09/05/2024. The time array has been adjusted, as previously explained, to account for the propagation from L1 to Earth. The first plot in Figure 4 shows that during the May 2024 storm, the maximum Dst index value was 61 nT, occurring 42 hours after midnight on May 9th. Conversely, the minimum value of -412 nT occurred 51 hours after midnight on May 9th. In all the plots, two vertical lines mark these specific times, indicating the beginning and end of the so-called "main phase" of the geomagnetic storm.

Before the onset of the geomagnetic storm, the Dst values remain relatively constant around zero. The peak corresponds to the sudden storm commencement (SSC), followed by a decrease in Dst values, marking the main phase until the minimum value is reached, indicating the storm's strength. After this point, the Dst index begins to rise again, signaling the recovery phase, which continues until normal values are restored. The vertical lines are added to all the plots to see the effects of the beginning and the ending of the storm in the other parameters that we calculated. The time shift we applied is in the x-axis of all plots except for Dst-index.

For the Alfvén speed (2nd plot in Figure 4), we observe that its values begin to increase before the 42-hour mark and continue rising. Around the middle of the main phase, there is a rapid drop, followed by another increase. After the storm ends, the Alfvén speed gradually decreases.

For the bulk speed (3rd plot in Figure 4), it initially remains nearly constant but starts increasing slightly before the 42-hour mark. During the main phase, the values remain elevated compared to the pre-storm period. However, after the storm, the bulk speed continues to increase. This suggests a clearer correlation at the onset of the storm.

For the Alfvénic Mach number (4th plot in Figure 4), we see that it is mostly $M_A < 1$, indicating a sub-Alfvénic plasma flow. A peak occurs around the 30-hour mark, briefly reaching a super-Alfvénic value of 1.08346. During the main phase of the storm, the Alfvénic Mach number remains low, and for the majority of the timeline, we observe sub-Alfvénic values.

The B_z/B_{tot} ratio (5th plot in Figure 4) exhibits significant variations. Between 28 and 33 hours, it reaches its minimum values and becomes negative. Then, before the 42-hour mark, we observe a steady increase, and it remains positive throughout the storm's duration.

Lastly, for the *y*-component of the convection electric field (last plot in Figure 4), we see near-zero values before the storm begins. During the main phase, the field increases, peaking at the end of the main phase before decreasing again with noticeable fluctuations.

Overall, these plots suggest that the SSC is associated with the compression of the magnetosphere due to the arrival of the high-speed stream at Earth. Additionally, the formation of ring currents and the corresponding decrease in the Dst index are directly linked to the intensification of the convection electric field.

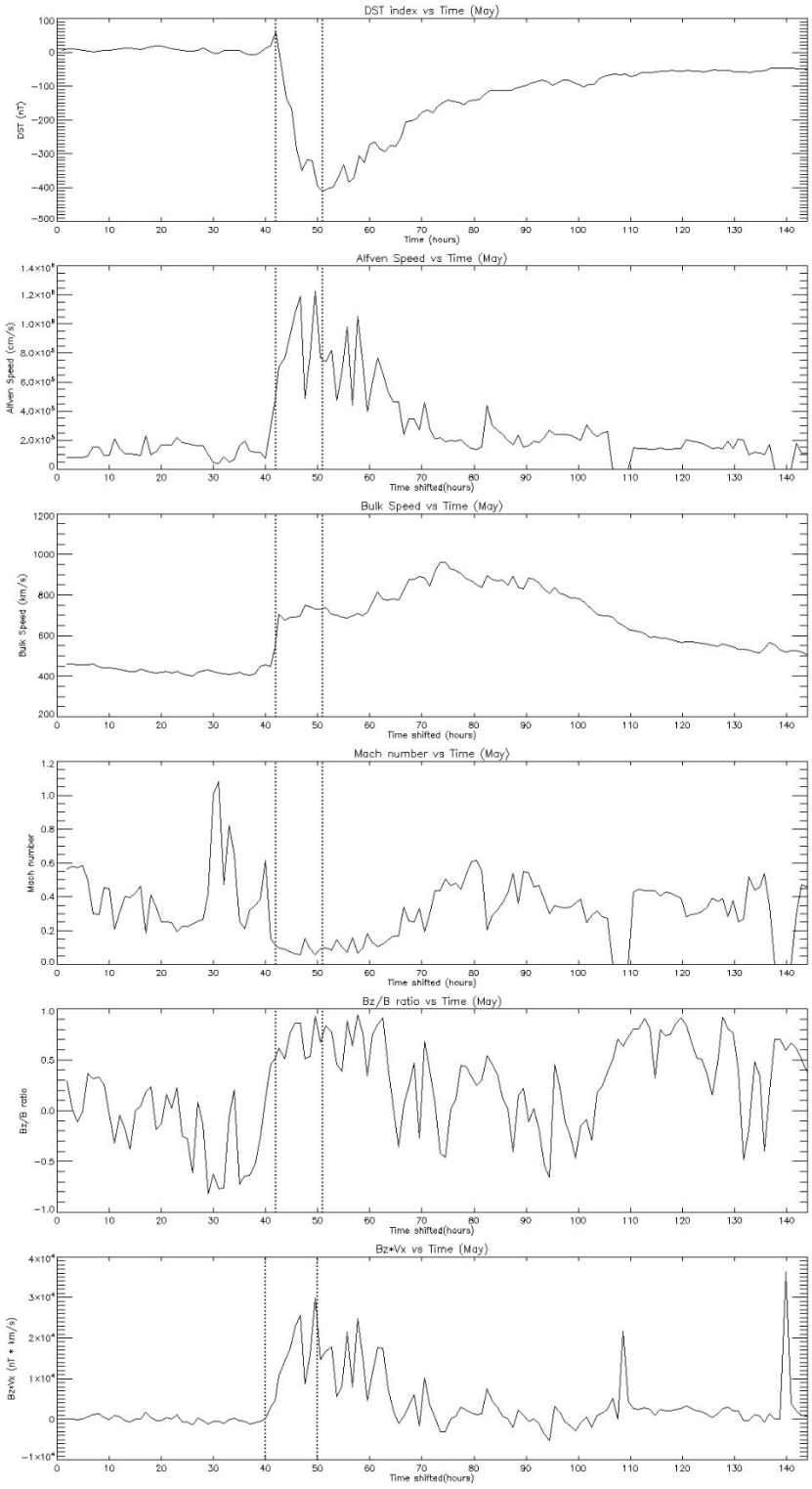

Figure 4: a summary of plasma properties and other parameters during the May 2024 geomagnetic storm. In detail, going from top to bottom: evolution of the Dst-index, of the Alfvén speed, bulk plasma speed, Alfvénic Mach number, ratio between the B_z component and the total magnetic field strength, and the E_y component of the convection electric field. With the exception of the plot showing the Dst-index, for all other plots the time axis has been shifted to account for the delay for the propagation of plasma from the Lagrangian point L1. In all plots the two vertical dotted lines denote the duration of the "main phase" of the geomagnetic storm.

4. The October 2024 storm

We followed the same approach for the geomagnetic storm of October 2024. As before, we added vertical lines at the maximum and minimum values of the Dst index to identify the main phase of the storm. The x-axis represents time in hours, with zero corresponding to 00:00 on 09/10/2024. Figure 5 provides all the plots for the October 2024 storm.

The Dst index reaches its maximum value of 49 nT at 40 hours, while the minimum value of -412 nT occurs at 50 hours. Unlike the May storm, the Dst values before the storm are not constant and close to zero. Instead, they suggest a recovery from a prior geomagnetic storm. As explained earlier, the vertical lines help identify the storm phases and facilitate comparisons with changes in other parameters.

For the Alfvén speed (2nd plot in Figure 5), we observe an increase immediately after hour 40, followed by a decrease starting a few hours before hour 50. Additional peaks appear later in the timeline, but they occur after the geomagnetic storm.

The bulk speed (3rd plot in Figure 5) increases sharply just before hour 40 as the storm arrives. During the main phase, it remains elevated and stable, similar to the May storm.

The Alfvénic Mach number (4th plot in Figure 5) again shows $M_A < 1$, indicating a sub-Alfvénic plasma flow. During the main phase of the storm, the values remain close to zero, consistent with the May event.

The B_z/B_{tot} ratio (5th plot in Figure 5) begins to increase rapidly a few hours before hour 40 and starts decreasing again at the beginning of the recovery phase. It remains positive throughout the storm's duration, except for a brief negative trough around hour 37, just before the storm.

Finally, the *y*-component of the convection electric field (6th plot in Figure 5) remains nearly constant at the beginning, then starts increasing just before hour 40. As the storm transitions from the main phase to the recovery phase, the field decreases again.

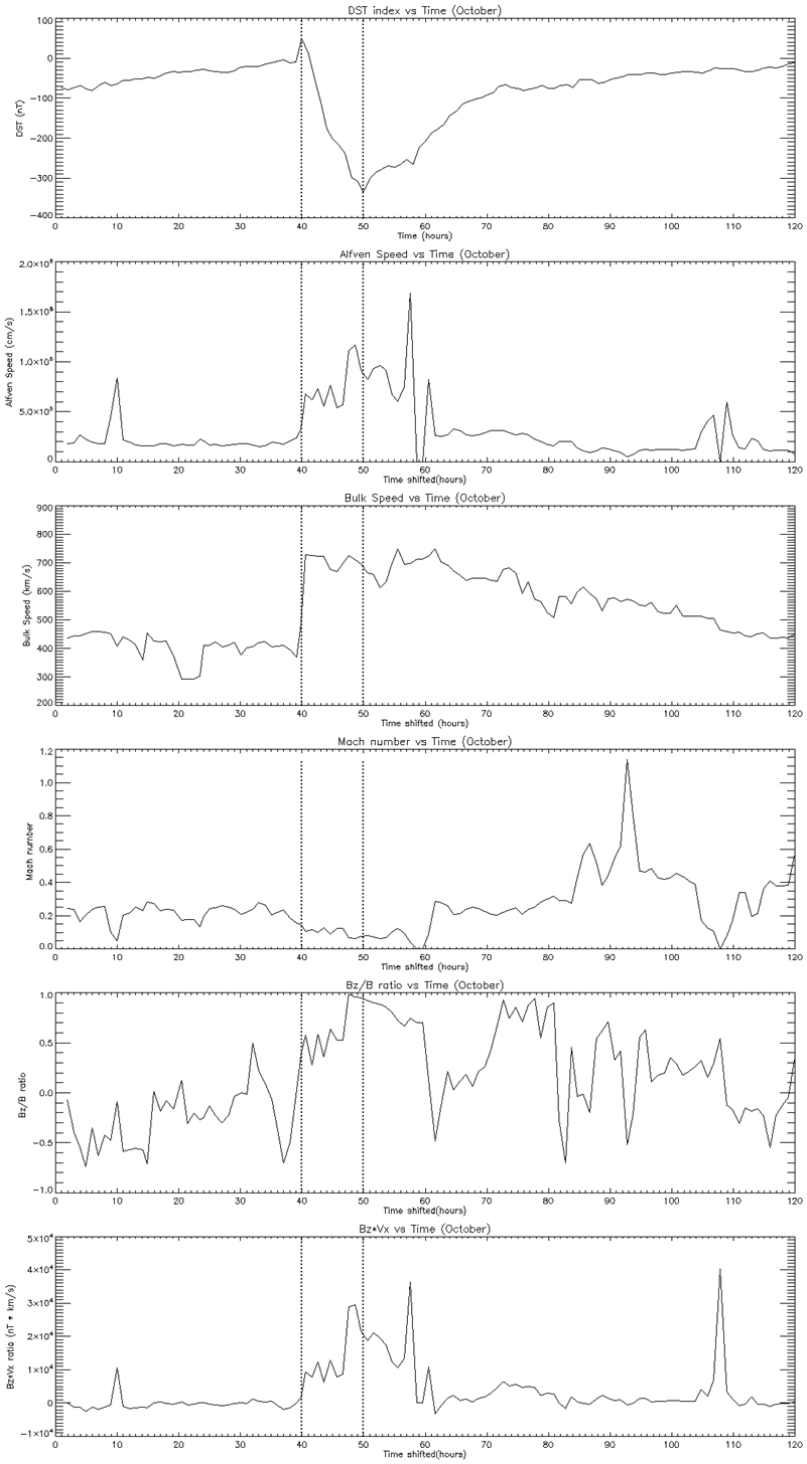

Figure 5: same as for the plots in the previous Figure, relative to the October 2024 geomagnetic storm.

5. Summary and conclusions

For the May geomagnetic storm, we observe a correlation between the Dst index and Alfvén speed. As the storm enters its main phase, the Alfvén speed shows a significant increase. The bulk speed also rises sharply when the Dst index reaches its maximum value. The Alfvénic Mach number remains very low due to the high Alfvén speed. The

B_z/B_{tot} ratio is positive during the main phase of the storm but becomes predominantly negative around hour 30. Lastly, the convection electric field increases suddenly during the main phase of the storm.

For the October geomagnetic storm, the correlation is stronger between the Dst index and bulk speed. While the sudden and significant changes in bulk speed may not occur at the exact same time as those in the Dst index, they are closely aligned, happening near the beginning and within the main phase of the storm. The Alfvén speed increases as the storm arrives and continues to rise throughout the main phase. During this period, the Alfvénic Mach number remains low, ranging between 0.0 and 0.2. Both the B_z/B_{tot} ratio and the convection electric field experience sudden increases during the storm, with the B_z/B_{tot} ratio reaching its minimum value at hour 37.

Acknowledgements

The work described here was performed during a two-months internship carried out in the framework of the ERASMUS project under an agreement between the Ioannina University and the INAF-Turin Astrophysical Observatory, in the period between mid-October and mid-December 2024.

Bibliography

Moldwin, M. (2008). Chapter 4. In *An introduction to space weather* (pp. 53–61). Cambridge University Press.

Notes from the course of *Solar Physics and Space Weather*, prof. Alessandro Bemporad, Department of Physics, University of Turin

Online references

Definition of space weather: *https://www.cost.eu/actions/724/*

Solar Monitor – Real-time solar activity. *https://www.solarmonitor.org*

SpaceWeather.com – News and information about the Sun-Earth environment. *https://spaceweather.com*

NOAA Space Weather Prediction Center (SWPC) *https://www.swpc.noaa.gov*

https://swelto.oato.inaf.it/in_situ_monitor.html